Available online at www.sciencedirect.com
SCIENCE DIRECT®
Carbohydrate Research 339 (2004) 2657–2665
Carbohydrate RESEARCH

Structure of minor oligosaccharides from the lipopolysaccharide fraction from *Pseudomonas stutzeri* OX1

Serena Leone,[a] Viviana Izzo,[b] Luisa Sturiale,[c] Domenico Garozzo,[c] Rosa Lanzetta,[a] Michelangelo Parrilli,[a] Antonio Molinaro[a,*] and Alberto Di Donato[b]

[a]*Dipartimento di Chimica Organica e Biochimica, Università degli Studi di Napoli Federico II, Via Cintia, 4, I-80126 Napoli, Italy*
[b]*Dipartimento di Chimica Biologica, Università degli Studi di Napoli Federico II, via Mezzocannone, 16, I-80134 Napoli, Italy*
[c]*Istituto per la Chimica e la Tecnologia dei Materiali Polimerici, ICTMP, CNR, Viale R. Margherita, 6, I-95123 Catania, Italy*

Received 18 June 2004; received in revised form 19 July 2004; accepted 9 September 2004
Available online 2 October 2004

Abstract—A minor oligosaccharide fraction was isolated after complete de-acylation of the lipooligosaccharide extracted from *Pseudomonas stutzeri* OX1. The full structure of this oligosaccharide was obtained by chemical degradation, NMR spectroscopy and MALDI-TOF MS spectrometry. These experiments showed the presence of two novel oligosaccharides (**OS1** and **OS2**):

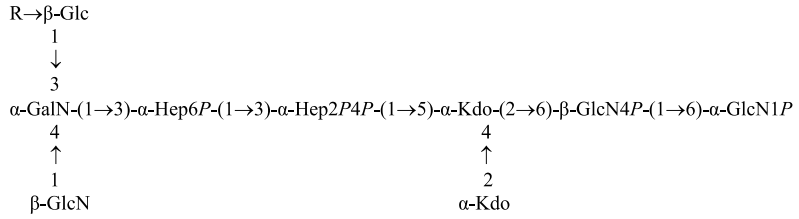

where R = (*S*)-Pyr(→4,6) in **OS1** and α-Rha-(1→3) in **OS2**. All sugars are D-pyranoses, except Rha, which is L-pyranose. Hep is L-*glycero*-D-*manno*-heptose, Kdo is 3-deoxy-D-*manno*-oct-2-ulosonic acid, Pyr is pyruvic acid, *P* is phosphate.

Keywords: *Pseudomonas stutzeri* OX1; Lipopolysaccharide; NMR spectroscopy; MALDI-TOF MS

1. Introduction

Pseudomonas stutzeri OX1 is a Gram-negative bacterium originally isolated from the activated sludge of a wastewater treatment plant,[1] where high concentrations of organic solvents are present. These conditions usually prohibit the survival of microorganisms because many enzymes are inactivated in the presence of organic solvents. However, a relatively small group of microorganisms is able to check these harmful effects because of peculiar biochemical features that allow their growth in harsh environmental conditions.

P. stutzeri OX1 is able to grow on a large spectrum of aromatics including phenol, cresols and dimethylphenols, on non-hydroxylated molecules as toluene, *o*-xylene[1] and benzene (Barbieri, personal communication). The microorganism is also capable to oxidize pollutants, like tetrachloroethylene (TCE), whose degradation, either with chemical or biological methods, is still very difficult.[2] Aerobic degradation of aromatic hydrocarbons by *P. stutzeri* is divided into an upper pathway, which produces dihydroxylated aromatic intermediates by the action of toluene-*o*-xylene monooxygenase (ToMO)[3–5] and/or phenol hydroxylase (PH),[6,7] and a

* Corresponding author. Tel.: +39 081 674124; fax: +39 081 674393; e-mail: molinaro@unina.it

0008-6215/$ - see front matter © 2004 Elsevier Ltd. All rights reserved.
doi:10.1016/j.carres.2004.09.006

lower pathway that processes these intermediates down to molecules that enter the citric acid cycle.[8]

The wide range of substrates that can be transformed by *P. stutzeri* invites applications ranging from bioremediation to regiospecific oxidation of hydrocarbons on an industrial scale. Recent studies have already indicated that cell membrane plays a central role in the adaptation mechanisms of Gram-negative bacteria to harsh environmental conditions, and in particular to organic solvents.[9,10] Generally, the survival of microorganisms depends on structural changes in outer and inner membranes,[11] that is, modifications of the fatty acids and phospholipids composition of the membrane itself, or on the development of extrusion mechanisms using vesicles, or on energy-dependent active efflux pumps, which export toxic organic solvents outside the cytoplasm.[9–11]

Lipopolysaccharides (LPSs) are the major components of the outer leaflet of the external Gram-negative bacterial membrane, which directly interact with the environment.[12] LPSs are typically made-up of three distinct structurally, chemically and biogenetically regions.[13] In their smooth form (S-LPSs), they include a glycolipid moiety, named lipid A, an oligosaccharide region (core), and a polysaccharide (O-specific chain, O-antigen), whereas in their rough form they are lipooligosaccharides (R-LPSs, LOSs) and lack the O-antigen. *P. stutzeri* OX1 synthesizes either LPSs or LOSs. We have already isolated and determined the structure of the major core oligosaccharide backbone from the LOS of *P. stutzeri* OX1,[14] which was found to possess a peculiar characteristic, that is, an unusual high number of negative charges in the outer leaflet of outer membrane. These charges are brought by the usual phosphate groups and by two pyruvic acid residues, to date never found in the core region of bacterial lipopolysaccharides.

In this paper, the complete and novel structure of two minor core oligosaccharides extracted from cells of *P. stutzeri* OX1 is described. These oligosaccharides were found to have closely related structures, similar also to that of other oligosaccharides already isolated.[13]

2. Results and discussion

The R-LPS was extracted from cells using the chloroform/petroleum ether/phenol method[15] and investigated by SDS-PAGE as described.[16] After silver staining,[16] typical migration pattern to the bottom of the gel was observed consistent with the low-molecular weight of a lipooligosaccharide. LOS was fully de-acylated by mild hydrazinolysis and strong alkaline hydrolysis. Sample was desalted on a Sephadex G-10 column and then lyophilized to give the core-lipid A oligosaccharide backbone. Compositional analysis of the oligosaccharide fraction by GC–MS of the acetylated methyl glycosides and alditol acetates derivatives yielded L,D-Hep, D-GalN, D-GlcN, D-Glc, Kdo and, in minor amount, L-Rha. Methylation analysis led to the identification of 3-substituted Hep, 6-substituted GlcN, 3,4-di-substituted GalN, terminal GlcN, 4,6-di-substituted Glc and, in lower amount, 3-substituted Glc and terminal Rha. Methylation analysis of the Kdo region led to the identification of 4,5-di-substituted Kdo and terminal Kdo.

The ^{1}H NMR spectrum (Fig. 1) showed eight major anomeric signals, corresponding to eight different spin systems (**A**–**H**). The residues, their linkages and their sequence were identified after a full 2D-NMR analysis (DQF-COSY, TOCSY, ROESY, NOESY, HSQC and HMBC) (Table 1). Anomeric and relative configurations were assigned on the basis of chemical shifts and ring proton $^{3}J_{H,H}$ values obtained from the DQF-COSY

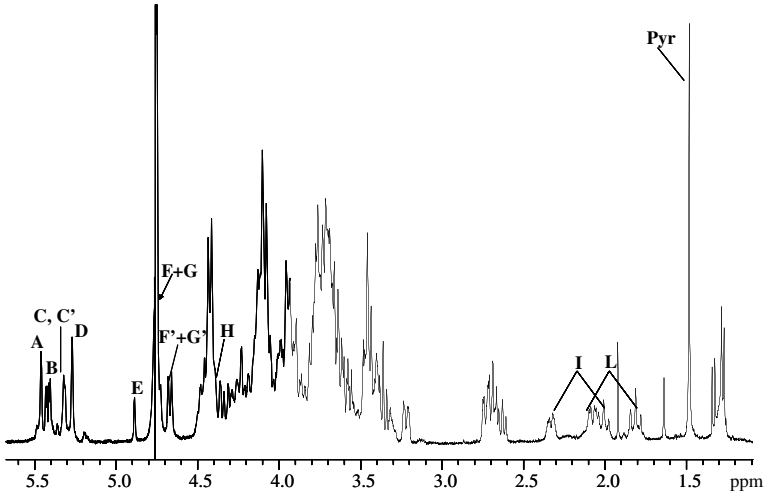

Figure 1. ^{1}H NMR spectrum and of oligosaccharides (**OS1** and **OS2**) obtained by alkaline degradation of the LOS from *P. stutzeri* OX1. Anomeric signals are indicated by capital letters.

Table 1. ^{1}H, ^{31}P and ^{13}C NMR chemical shifts (ppm) measured at 30 °C and pD 14 of de-acylated lipopolysaccharide from *P. stutzeri* OX1

	1(H-3_{ax})	2(H-3_{eq})	3(4)	4(5)	5(6)	6(7)	7(8)
OS1							
A	5.46	4.40	4.10	4.41	4.14	4.20	3.87
3-α-Hep I	97.6	74.0	74.2	72.7	71.3	69.2	63.7
		−0.39		0.94			
B	5.42	2.72	3.63	3.44	4.09	4.32/3.74	
6-α-GlcN	94.9	55.7	73.6	70.4	72.1	70.0	
		−1.0					
C	5.31	3.21	4.07	4.36	4.11	4.09	
3,4-α-GalN	101.4	51.2	81.4	76.2	71.6	63.0	
D	5.26	4.42	4.15	4.05	3.95	4.47	3.73/3.78
3-α-Hep II	102.5	69.7	77.9	71.4	72.7	72.2	62.8
						1.36	
F	4.73	3.45	3.96	3.44	3.48	3.68/4.09	
t-β-Glc	105.5	75.0	74.7	76.3	66.5	64.8	
G	4.74	2.68	3.39	3.45	3.33	3.76	
t-β-GlcN	104.4	57.3	76.7	70.4	76.5	61.2	
H	4.42	2.68	3.58	3.64	3.68	3.78/3.45	
6-β-GlcN	103.2	57.5	76.5	74.4	74.5	63.4	
				0.26			
I	2.00	2.32	4.10	4.23	3.69	3.96	3.92/3.65
4,5-α-Kdo	34.8		67.6	67.3	73.3	69.3	64.1
L	1.81	2.07	4.27	4.10	3.71	3.94	3.94/3.75
t-α-Kdo	35.8		65.9	66.1	73.1	69.4	63.0
OS2							
C′	5.31	3.21	4.09	4.42	4.11	4.09	
3,4-α-GalN	101.4	51.2	80.9	77.1	71.6	63.0	
E	4.88	4.00	3.78	3.46	4.06	1.28	
t-α-Rha	101.3	70.7	70.6	72.7	69.4	16.8	
F′	4.66	3.39	3.62	3.53	3.71	3.80	
3-β-Glc	105.0	74.3	77.6	75.2	73.1	60.9	
G′	4.67	2.62	3.35	3.38	3.31	3.74/3.91	
t-β-GlcN	103.4	57.2	76.6	70.3	76.3	61.2	

Chemical shifts for the pyruvic acid residue are 1.48/25.1, 102.1 and 175.6 ppm, respectively. In brackets are indicated the nuclei of Kdo residues.

spectrum. All sugar residues were present as pyranose rings, according to either ^{13}C chemical shift values or to the occurrence of long-range correlations between C-1/H-1 and H-5/C-5 in the $^{1}H,^{13}C$ HMBC spectrum (for Kdo residues between C-2 and H-6). In particular, five residues (**A**–**E**) were in α-configuration, whereas the other three (residues **F**–**H**) were in β-configuration. This was also supported by a ROESY experiment that showed intra-residual NOE connectivity from H-1 to H-3 and to H-5 for residues **F**–**H**. The ^{31}P NMR spectrum gave evidence for the presence of five different monophosphate ester groups in the range of chemical shift between −1.00 and 1.36 ppm.

Anomeric resonances of the spin systems **A** and **D** were both present as singlet signals, with a $^{3}J_{1,2} <$ 2 Hz. From H-2 of both residues it was possible to identify in the TOCSY spectrum all the other resonances of ring protons. Furthermore, the connectivity between H-5 and H-6 of both spin systems was also confirmed by their dipolar contacts showed by ROESY spectrum, leading to the identification of these residues (**A** and **D**) as two α-heptoses. Chemical shift values for H-2**A**, H-4**A** and H-6**D** (4.40, 4.41 and 4.47 ppm) were indicative of *O*-phosphorylation at these sites. This was also confirmed by the existence of cross peaks in the $^{1}H,^{31}P$ HSQC spectrum with signals at −0.39, 0.94 and 1.36 ppm, respectively (Fig. 2).

Anomeric signal H-1**B** was present as double doublet with a $^{3}J_{H\text{-}1,H\text{-}2} = 3.1$ Hz, and a $^{3}J_{H\text{-}1,P} = 8.9$ Hz. The *O*-phosphorylation at the anomeric position was confirmed by the presence of a cross peak at 5.42/−1.00 ppm in the $^{1}H,^{31}P$ HSQC spectrum. The resonance of C-2**B** at 55.7 ppm of a nitrogen-bearing carbon indicated that **B** was a 2-deoxy-2-amino residue. On the basis of the $^{3}J_{H,H}$ values, characteristic of α-*gluco* configuration, it was deduced that residue **B** was the α-GlcN of the lipid A backbone. Residue **C**, a *galacto*-configurated monosaccharide, possessed the typical small $^{3}J_{H\text{-}3,H\text{-}4}$ and $^{3}J_{H\text{-}4,H\text{-}5}$ values (3 and 1 Hz, respectively). Thus, H-5 resonance was definitely established by NOE effect with H-4 in the ROESY spectrum. The signal for C-2 at 51.2 ppm indicated the presence of a nitrogen-bearing carbon, making possible the identification of spin system **C** as α-GalN. A singlet signal, present in non-stoichiometric ratio (H-1**E**, 4.88 ppm), was identified as the anomeric proton of a α-*manno*-configured monosaccharide. In addition, it correlated to a methyl signal at 1.28 ppm in the TOCSY spectrum, thus, it was identified as the

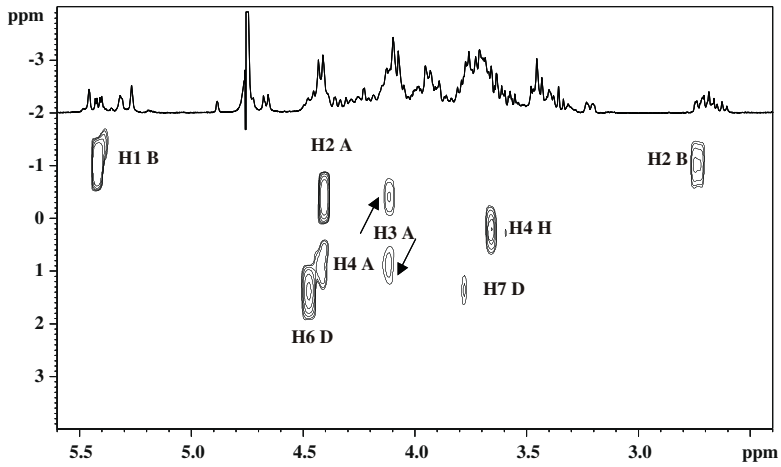

Figure 2. The $^{1}H,^{31}P$ HSQC spectrum of oligosaccharides (**OS1** and **OS2**) obtained by alkaline degradation of the LOS from *P. stutzeri* OX1 in which all the relevant heteronuclear $^{3}J_{P,H}$ and $^{4}J_{P,H}$ correlations are visible. The ^{1}H NMR spectrum is also visible within the figure.

α-Rha residue. The spin system **H** ($^{3}J_{H\text{-}1,H\text{-}2} = 8.0$ Hz) was identified as the β-GlcN of lipid A backbone on the basis of its ring protons chemical shifts and coupling constants (in the range of 10 Hz) and because H-2 signal correlated to a nitrogen-bearing carbon signal in the HSQC spectrum (57.5 ppm).

The signal at 4.74 ppm was assigned to two β-anomeric protons of two *gluco*-configured residues (H-1**F** and H-1**G**), as confirmed by DQF-COSY spectrum in which two different cross peaks were present (4.73/3.45 ppm, H-1**F**/H-2**F** and 4.74/2.68 ppm, H-1**G**/H-2**G**) and by $^{3}J_{H,H}$ ring proton values about 11 Hz for both spin systems. Residue **F** was identified as β-Glc, whereas residue **G** as β-GlcN, given the chemical shift of C-2**G**, 57.3 ppm, typical of a nitrogen-bearing carbon. Besides these major signals, a minor set of signals was present, namely, a doublet relative to two anomeric protons. The corresponding spin systems (**F**′ and **G**′) belonged to the minor oligosaccharide, and could be identified as a β-Glc (**F**′) and a β-GlcN (**G**′), on the basis of the same considerations made for **F** and **G**.

In the high-field region of the ^{1}H NMR spectrum the typical signals of two diastereotopic methylene groups of two Kdo residues (**I** and **L**) were visible, at 2.00/2.33 and 1.81/2.07 ppm. All resonances of Kdo residues were assigned by COSY, TOCSY and ROESY. In particular, the ROESY experiment was useful for the identification of H-6 resonance of both residues, given the very low $^{3}J_{H\text{-}5,H\text{-}6}$ value (less than 1 Hz). Their α-configuration was established on the basis of the chemical shifts of the H-3_{eq} and H-5 protons and by the values of the $^{3}J_{H\text{-}7,H\text{-}8a}$ and $^{3}J_{H\text{-}7,H\text{-}8b}$ coupling constants of 7.2 and 3.1 Hz, respectively.[17,18]

Moreover, in the high-field region of ^{1}H NMR spectrum a singlet methyl group belonging to a pyruvic acid residue was visible at 1.48 ppm. The nature of this substituent was confirmed by presence of correlations, in the $^{1}H,^{13}C$ HMBC spectrum, with carbons at 102.1 and 175.6 ppm.

The ^{13}C NMR chemical shifts (Table 1) could be assigned by a HSQC experiment, using the assigned proton resonances. Anomeric signals were apparent (Fig. 3), beside a large number of carbon signals relative to ring carbon, few nitrogen-bearing carbon signals and, in addition, at high fields, the two methylene carbon signal of Kdo units and the methyl carbon signal of pyruvic moiety were found. Low-field shifted carbon signals indicated substitution at O-3 of **A**, **D** and **F**′, O-6 of **B** and **H**, O-3 and O-4 of **C** and **C**′, O-4 and O-5 of **I**, O-4 and O-6 of **F**, whereas **G**, **G**′, **E** and **L** were terminal residues.[19]

The connectivity among residues and their sequence in both the oligosaccharide chains were inferred by NOE correlations found in the ROESY spectrum (Fig. 4), methylation analysis, ^{13}C NMR glycosylation shift data and, eventually, scalar long-range correlations in the $^{1}H,^{13}C$ HMBC spectrum (not shown). The typical lipid A backbone, composed by residues **B** and **H**, was present, as confirmed by NOE correlation between H-1**H** and H-6**B**. In the case of Kdo unit **I**, it was substituted at O-5 by heptose **A** as suggested by the NOE contacts found between H-1**A** and H-5 and H-7**I**, and, in addition, between H-5**A** and H-3_{ax}**I**. Kdo **I** was further substituted at O-4 by terminal Kdo **L** as demonstrated by the NOE effect between H-6**L** and H-3_{eq}**I**. These NOE data and the information on absolute configuration of heptose **A** also gave evidence for the absolute configuration of residues **I** and **L**, and for the sequence of the typical inner core backbone of *Pseudomonas* LPS, built-up of α-L,D-Hep-(1→5)-[α-D-Kdo-(2→4)]-α-D-Kdo.[20,21] Heptose **A** was, in turn, substituted at O-3 by heptose **D** as shown by the NOE effect between anomeric signal H-1**D** and H-3**A**. The NMR signals for the monosaccharides described above showed no hetero-

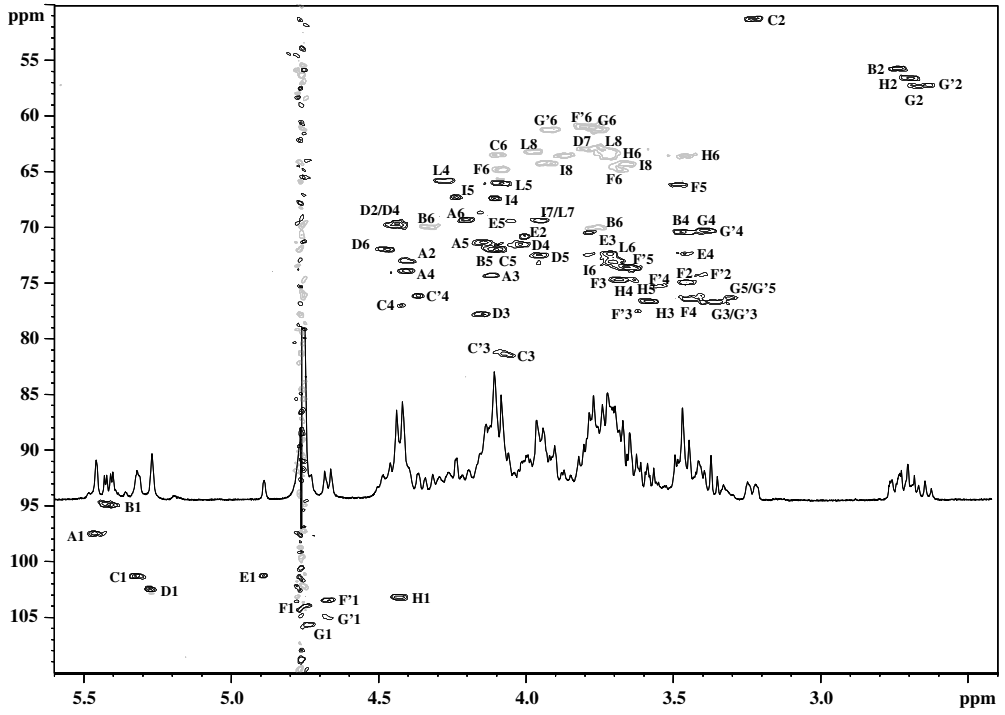

Figure 3. The $^{1}H,^{13}C$ HSQC spectrum of oligosaccharides (**OS1** and **OS2**) obtained by alkaline degradation of the LOS from *P. stutzeri* OX1 in which all the heteronuclear correlations are assigned. Experiment was carried out with carbon multiplicity editing, in the phase-sensitive mode and the data matrix was extended using forward linear prediction extrapolation. Grey cross peaks refer to CH_2 carbon. The ^{1}H NMR spectrum is sketched within the figure.

geneity, in agreement with a common inner core structure for both oligosaccharides.

Residues **C** and **C′** (α-GalN) were attached at O-3 of Hep **D** in the two oligosaccharides **OS1** and **OS2**, respectively, as indicated by the strong NOE effects H-1**C**/**C′** H-3**D**. The minor series of signals (**C′**) from the α-GalN spin system differed in chemical shifts of H-3 and H-4 signals (Table 1). This was in agreement with a different glyco-substitution of this residue in **OS1** and **OS2**.

In the major oligosaccharide (**OS1**) residues **F** and **G**, were linked to residue **C** to O-3 and O-4, respectively, as shown by NOE correlations H-1**F**-H-3**C** and H-1**G**-H-4**C**. According to chemical shift values for proton and carbon, residue **G** (GlcN) was unsubstituted, whereas residue **F** (Glc), showed a weak downfield shift of carbon resonances for C-4 and C-6. In agreement, a considerable downfield displacement of resonances for H-6_a and H-6_b, of residue **F** was detectable, as well. This was caused by substitution at O-4 and O-6 of residue **F** of pyruvic acid as a cyclic ketal, as concluded by a scalar long-range correlation found in the HMBC spectrum between C-2 of pyruvic acid and H-4 and H-6 of **F**. The lack of any strong NOE effect between the methyl group of the pyruvate residue and the **F** ring proton signals, indicated an equatorial orientation for methyl group in a chair-like conformation of the ketal, hence the *S*-configuration at C-2 of pyruvate. This hypothesis was confirmed by the ^{1}H and ^{13}C chemical shifts of pyruvate residue that are highly diagnostic of its absolute configuration.[22]

The MALDI-TOF spectrum (Fig. 5) of the de-acylated oligosaccharide confirmed the structural assignments. The main ion peak, at *m/z* 2118.4, was identified as **OS1** oligosaccharide, composed by the following residues: two Kdo, two Hep, one Hex, four HexN, five phosphate groups and a pyruvic acid residue.

In conclusion, the structure of **OS1** can be described as it follows:

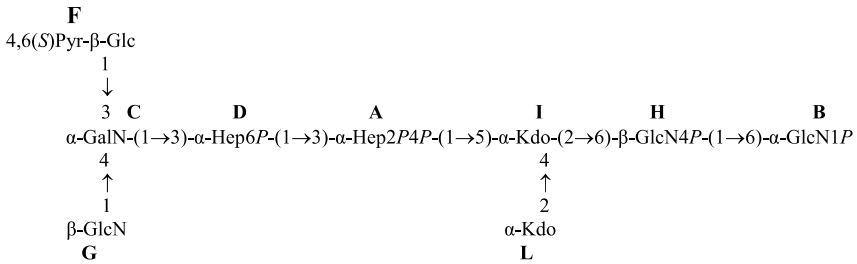

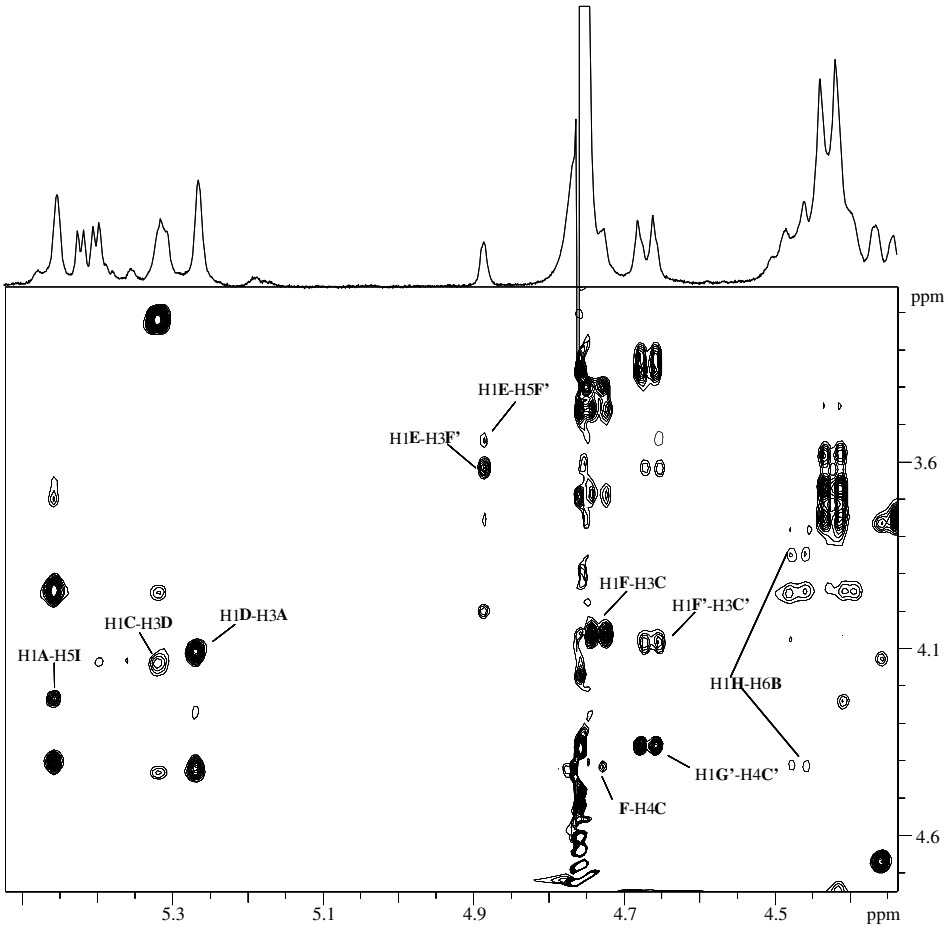

Figure 4. Section of the antiphase ROESY and ^{1}H NMR spectra of oligosaccharides (**OS1** and **OS2**). Annotations refer to interresidual cross peaks. The capital letters refer to residues as denoted in Table 1.

As already concluded before, the inner core region of the minor oligosaccharide **OS2** has the same structure of **OS1**, but the outer core differs for the presence of an extra rhamnose residue substituting the Glc residue (**F′**) at O-3. This was indicated by the downfield displacement of C-3**F′** resonance (77.6 ppm), by the NOE H-1**E**-H-3**F′**, and by a correlation in the $^{1}H,^{13}C$ HMBC spectrum between H-1**E** and C-3**F′**. Residue **G′** still was a terminal GlcN, and the small differences observed in proton and carbon resonances were probably due to different magnetic environment because of substitution on **F′**. Also in this case, this structural assignment was positively confirmed by the MALDI-MS data (Fig. 5) in which a second ion peak at *m/z* 2194.5 was present, confirming the structure of the **OS2** oligosaccharide below:

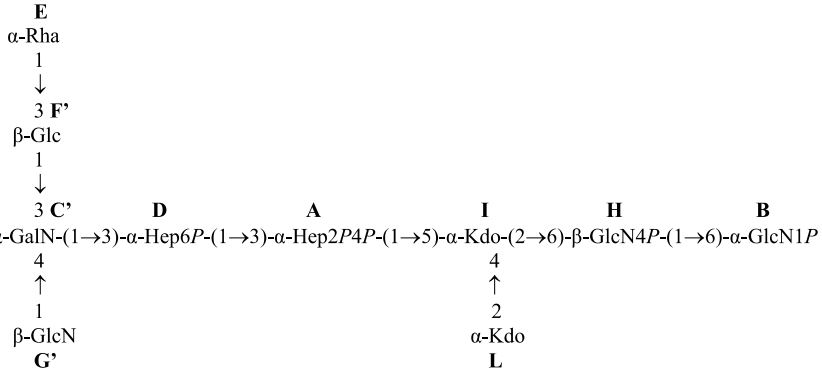

It should be underlined that both the **OS1** and **OS2** structures differ from that already described for the major

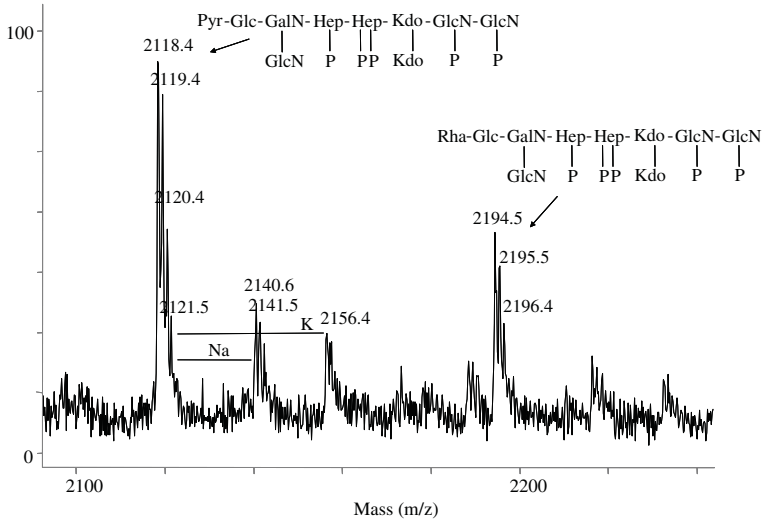

Figure 5. Negative ion MALDI-TOF mass spectrum of oligosaccharide (**OS1** and **OS2**) obtained in reflector mode. Assignments of ion peaks are shown. Abbreviations: P is phosphate, Pyr is pyruvic acid.

oligosaccharide from the LOS of *P. stutzeri* OX1[14] in the absence of a pyruvic acid residue on the terminal GlcN residue (**G** and **G′**, see the formula). In the case of the **OS1** structure, the only difference from the major oligosaccharide[14] is the lack of the pyruvic acid ketal on **G** residue and we cannot exclude the fact that this product can be derived by the cleavage of the ketal group in the course of LOS isolation, although ketal linkage is generally not sensitive to alkaline conditions.

In addition, the pyruvic acid substituent on Glc residue (**F′**) is also missing in the **OS2** structure, which is different from **OS1** and the major oligosaccharide structures and represents another core glycoform.[14] In fact, **OS2** bears an additional Rha residue at its O-3**F′** position, which, in all *Pseudomonas*, is the typical substrate for chain elongation. This would suggest that the pyruvate residue is used to block chain elongation in the LOS of *P. stutzeri* OX1, as we already suggested.[14]

3. Experimental

3.1. Bacterial growth and LPS extraction

Cells were routinely grown on M9-agar plates supplemented with 10 mM malic acid as the sole carbon source, at 27 °C. For growth in liquid medium a single colony from a fresh plate was inoculated in 1 mL of the medium and grown overnight at 27 °C under constant shaking. This saturated culture was used to inoculate 100 mL of the same medium and grown at 27 °C up to about 1 OD_{600}. Final growth was started by inoculating the appropriate volume of the latter culture into 1 L of fresh medium to 0.02 OD_{600}. Cells were grown at 27 °C, until $OD_{600} = 1$ was reached and recovered by centrifugation at 3000*g*, for 15 min, at 4 °C, washed with an isotonic buffer and lyophilized. Growth was carried out in rich LB medium and dried cell yields was 0.21 g/L. Dried bacterial cells were extracted in aqueous 90% phenol/chloroform/petroleum ether (50 mL, 2:5:8 v/v/v) as described.[15] After removal of the organic solvents under vacuum, the LOS fraction was precipitated from phenol with water, washed first with aqueous 80% phenol, and then three times with cold acetone. Each time the sample was centrifuged and finally lyophilized (92 mg, yield: 4.4% of bacterial dry mass). Sodium dodecyl sulfate polyacrylamide gel electrophoresis (SDS-PAGE) was performed as described.[16] For detection of LOS, gel was stained with silver nitrate.[16]

3.2. General and analytical methods

Determination of Kdo, neutral sugars, including the determination of the absolute configuration of the heptose residues, organic bound phosphate, absolute configuration of the hexoses, GLC and GLC–MS were all carried out as described.[23–26] For methylation analysis of Kdo region, LOS was carboxy-methylated with methanolic HCl (0.1 M, 5 min) and then with diazomethane to improve its solubility in DMSO. Methylation was carried out as described.[27,28] LOS was hydrolyzed with 2 M trifluoroacetic acid (100 °C, 1 h), carbonyl reduced with $NaBD_4$, carboxy-methylated as described above, carboxyl reduced with $NaBD_4$ (4 °C, 18 h), acetylated and analyzed by GLC–MS. Methylation of the complete core region was carried out as described.[29] The sample was hydrolyzed with 4 M trifluoroacetic acid (100 °C,

4 h), carbonyl reduced with $NaBD_4$, acetylated and analyzed by GLC–MS.

3.3. Isolation of oligosaccharides

An aliquot of LOS (50 mg) was dissolved in anhydrous hydrazine (2 mL), stirred at 37 °C for 90 min, cooled, poured into ice-cold acetone (20 mL) and allowed to precipitate. The precipitate was then centrifuged (3000*g*, 30 min), washed twice with ice-cold acetone, dried, dissolved in water and lyophilized (40 mg, 80% of the LOS). This material was de-*N*-acylated with 4 M KOH as described.[30] Salts were removed using a Sephadex G-10 (Pharmacia) column (50 × 1.5 cm). The resulting oligosaccharide constitutes the complete carbohydrate backbone of the lipid A-core region (20 mg, 40% of the LOS).

3.4. NMR spectroscopy

For structural assignments of oligosaccharides, 1D and 2D ^1H NMR spectra were recorded on a solution of 5 mg in 0.6 mL of D_2O, at 30 °C, at pD 14 (uncorrected value). ^1H and ^{13}C experiments were carried out using a Varian Inova 500 instrument whereas for ^{31}P NMR spectra a Bruker DRX-400 spectrometer was used. Spectra were calibrated with internal acetone (δ_H 2.225, δ_C 31.45). Aqueous 85% phosphoric acid was used as external reference (δ_P 0.00) for ^{31}P NMR spectroscopy. Nuclear Overhauser enhancement spectroscopy (NOESY) and rotating frame Overhauser enhancement spectroscopy (ROESY) were measured using data sets ($t_1 \times t_2$) of 4096 × 1024 points, and 16 scans were acquired. A mixing time of 200 ms was used. Double quantum-filtered phase-sensitive COSY experiments were performed with 0.258 s acquisition time, using data sets of 4096 × 1024 points, and 64 scans were acquired. Total correlation spectroscopy experiments (TOCSY) were performed with a spinlock time of 80 ms, using data sets ($t_1 \times t_2$) of 4096 × 1024 points, and 16 scans were acquired. In all homonuclear experiments the data matrix was zero-filled in the *F*1 dimension to give a matrix of 4096 × 2048 points and was resolution enhanced in both dimensions by a shifted sine-bell function before Fourier transformation. Coupling constants were determined on a first-order basis from 2D phase-sensitive double quantum-filtered correlation spectroscopy (DQF-COSY).[31,32] Heteronuclear single quantum coherence (HSQC) and heteronuclear multiple bond correlation (HMBC) experiments were measured using pulse field gradient programs in the ^1H-detected mode via single quantum coherence with proton decoupling in the ^{13}C domain, using data sets of 2048 × 512 points, and 64 scans were acquired for each t_1 value. Experiments were carried out in the phase-sensitive mode according to the method of States et al.[33] The ^1H,^{13}C HSQC experiment was carried out with carbon multiplicity editing. A 60 ms delay was used for the evolution of long-range connectivity in the HMBC experiment. In all heteronuclear experiments the data matrix was extended to 2048 × 1024 points using forward linear prediction extrapolation.[34,35]

3.5. MALDI-TOF analysis

MALDI mass spectra were carried out in the negative polarity in reflector mode on a Voyager STR instrument (Applied Biosystems, Framingham, MA, USA) equipped with a nitrogen laser (λ = 337 nm) and provided with delayed extraction technology. Ions formed by the pulsed laser beam were accelerated through 24 kV. Each spectrum is the result of approximately 200 laser shots. Saturated solution of 2,4,6-trihydroxyacetophenone (THAP) was used as the matrix.

Acknowledgements

This work was supported by grants (to A.D.D. and M.P.) from the Ministry of University and Research (PRIN/2000 and PRIN/2002). NMR experiments were carried out on a 500 MHz spectrometer of Consortium INCA (L488/92, Cluster 11) at Centro Interdipartimentale Metodologie Chimico Fisiche Università di Napoli.

References

1. Baggi, G.; Barbieri, P.; Galli, E.; Tollari, S. *Appl. Environ. Microbiol.* **1987**, *53*, 2129–2132.
2. Ryoo, D.; Shim, H.; Canada, K.; Barbieri, P.; Wood, T. K. *Nat. Biotechnol.* **2000**, *18*, 775–778.
3. Cafaro, V.; Scognamiglio, R.; Viggiani, A.; Izzo, V.; Passaro, I.; Notomista, E.; Piaz, F. D.; Amoresano, A.; Casbarra, A.; Pucci, P.; Di Donato, A. *Eur. J. Biochem.* **2002**, *69*, 5689–5699.
4. Bertoni, G.; Martino, M.; Galli, E.; Barbieri, P. *Appl. Environ. Microbiol.* **1998**, *64*, 3626–3632.
5. Sazinsky, M. H.; Bard, J.; Di Donato, A.; Lippard, S. J. *J. Biol. Chem.* **2004**, *279*, 30600–30610.
6. Arenghi, F. L.; Berlanda, D.; Galli, E.; Sello, G.; Barbieri, P. *Appl. Environ. Microbiol.* **2001**, *67*, 3304–3308.
7. Cafaro, V.; Izzo, V.; Scognamiglio, R.; Notomista, E.; Capasso, P.; Casbarra, A.; Pucci, P.; Di Donato, A. *Appl. Environ. Microbiol.* **2004**, *70*, 2211–2219.
8. Powlowski, J.; Shingler, V. *J. Bacteriol.* **1990**, *172*, 6834–6840.
9. Ramos, J. L.; Gallegos, M. T.; Marqués, S.; Ramos-Gonzàlez, M. I.; Espinosa-Urgel, M.; Segura, A. *Curr. Opin. Microbiol.* **2001**, *4*, 166–171.
10. Ramos, J. L.; Duque, E.; Rodríguez-Herva, J. J.; Godoy, P.; Haidour, A.; Reyes, F.; Fernandez- Barrero, A. *J. Biol. Chem.* **1997**, *272*, 3887–3890.
11. Ramos, J. L.; Duque, E.; Gallegos, M. T.; Godoy, P.; Ramos-Gonzalez, M. I.; Rojas, A.; Téran, W.; Segura, A. *Annu. Rev. Microbiol.* **2002**, *56*, 743–767.

12. Alexander, C.; Rietschel, E. Th. *J. Endotoxin Res.* **2001**, *7*, 167–202.
13. Holst, O. In *Endotoxin in Health and Disease*; Brade, H., Morrsion, D. C., Opal, S., Vogel, S., Eds.; Marcel Dekker: New York, 2002; pp 115–154.
14. Leone, S.; Izzo, V.; Silipo, A.; Sturiale, L.; Garozzo, D.; Lanzetta, R.; Parrilli, M.; Molinaro, A.; Di Donato, A. *Eur. J. Biochem.* **2004**, *271*, 2691–2704.
15. Galanos, C.; Lüderitz, O.; Westphal, O. *Eur. J. Biochem.* **1969**, *9*, 245–249.
16. Kittelberger, R.; Hilbink, F. *J. Biochem. Biophys. Methods* **1993**, *26*, 81–86.
17. Birnbaum, G. I.; Roy, R.; Brisson, J. R.; Jennings, H. *J. Carbohydr. Chem.* **1987**, *6*, 17–39.
18. Holst, O.; Thomas-Oates, J. E.; Brade, H. *Eur. J. Biochem.* **1994**, *222*, 183–194.
19. Lipkind, G. M.; Shashkov, A. S.; Knirel, Y. A.; Vinogradov, E. V.; Kochetkov, N. K. *Carbohydr. Res.* **1988**, *175*, 59–75.
20. Holst, O.; Bock, K.; Brade, L.; Brade, H. *Eur. J. Biochem.* **1995**, *229*, 194–200.
21. Bock, K.; Vinogradov, E. V.; Holst, O.; Brade, H. *Eur. J. Biochem.* **1994**, *225*, 1029–1039.
22. Garegg, P. J.; Jansson, P. E.; Lindberg, B.; Lindh, F.; Lonngren, J. *Carbohydr. Res.* **1980**, *16*, 127–132.
23. Vinogradov, E. V.; Holst, O.; Thomas-Oates, J. E.; Broady, K. W.; Brade, H. *Eur. J. Biochem.* **1992**, *210*, 491–498.
24. Kaca, W.; de Jongh-Leuvenink, J.; Zähringer, U.; Brade, H.; Verhoef, J.; Sinnwell, V. *Carbohydr. Res.* **1998**, *179*, 289–299.
25. Holst, O.; Broer, W.; Thomas-Oates, J. E.; Mamat, U.; Brade, H. *Eur. J. Biochem.* **1993**, *214*, 703–710.
26. Süsskind, M.; Brade, L.; Brade, H.; Holst, O. *J. Biol. Chem.* **1998**, *273*, 7006–7017.
27. Ciucanu, I.; Kerek, F. *Carbohydr. Res.* **1984**, *131*, 209–217.
28. Hakomori, S. *J. Biochem. (Tokyo)* **1964**, *55*, 205–208.
29. Molinaro, A.; De Castro, C.; Lanzetta, R.; Evidente, A.; Parrilli, M.; Holst, O. *J. Biol.Chem.* **2002**, *277*, 10058–10063.
30. Holst, O. In *Methods in Molecular Biology, Bacterial Toxins: Methods and Protocols*; Holst, O., Ed.; Humana: Totowa, NJ, 2000; pp 345–353.
31. Piantini, U.; Sørensen, O. W.; Ernst, R. R. *J. Am. Chem. Soc.* **1982**, *104*, 6800–6801.
32. Rance, M.; Sørensen, O. W.; Bodenhausen, G.; Wagner, G.; Ernst, R. R.; Wüthrich, K. *Biochem. Biophys. Res. Commun.* **1983**, *117*, 479–485.
33. States, D. J.; Haberkorn, R. A.; Ruben, D. J. *J. Magn. Reson.* **1982**, *48*, 286–292.
34. de Beer, R.; van Ormondt, D. *NMR-Basic Princ. Prog.* **1982**, *26*, 201.
35. Hoch, J. C.; Stern, A. S. In *NMR Data Processing*; Hoch, J. C., Stern, A. S., Eds.; Wiley: New York, 1996; pp 77–101.